

Sensitivity of Analysis and Forecast RMSE to ETKF Observation Filtering in the GSI/ETKF Regional Hybrid

Arthur P. Mizzi¹

NCAR Earth System Laboratory
Mesoscale and Microscale Meteorology Division
Boulder, CO 80307

1. Introduction

Recently, there has been much interest in hybrid variational data assimilation research. *See e.g.*, Wang 2010, Bowler et al. 2008, and Wang et al. 2008a, b. This paper continues that research by extending the work of Wang et al. 2008a, b to a regional version of the NOAA Gridpoint Statistical Interpolation (GSI) global hybrid assimilation scheme described by Wang 2010. For this research, the NOAA Environmental Modeling Center (EMC), in collaboration with the University of Oklahoma, developed the GSI global hybrid code. We modified that code to incorporate an ETKF interface and apply the GSI/ETKF hybrid in a regional setting with WRF-ARW.

2. The GSI/ETKF hybrid scheme

The GSI/ETKF regional hybrid cycling algorithm follows that of Wang et al. 2007. We start with an ensemble of background forecasts. The assimilation cycle begins by calculating the ensemble mean and perturbations. It proceeds by updating the mean with the GSI/ETKF regional hybrid and updating the perturbations with the ETKF. The mathematical formalism is identical to that of Wang et al. 2008a. The ETKF uses the method described by Bishop et al. 2001 with the inflation factor strategy described by Wang et al. 2007. For the ETKF, we use an averaging period of 10 days.

After updating the ensemble mean and perturbations, we reconstitute the total fields for each ensemble member, update the boundary conditions, and use WRF/ARW to make 12-hr forecasts for each ensemble member. Those forecasts become the background forecasts for the next cycle, and the assimilation process is repeated.

For a more detailed discussion of the GSI/ETKF regional hybrid and the experimental design underlying the work reported here, *see* Mizzi et al. 2011.

3. The ETKF

In the GSI/ETKF regional hybrid, the ETKF creates ensemble spread to represent the forecast distribution resulting from observation uncertainty with the goal of increasing the ensemble mean forecast accuracy. However, the disparity between the ensemble size (relatively small) and the number of observations entering the ETKF (relatively large)

¹ Corresponding author: Arthur P. Mizzi, NCAR/MMM P.O. Box 3000, Boulder, CO., mizzi@ucar.edu, 303-903-5544.

causes the ETKF to misrepresent the ensemble spread.² Inflation factors are commonly used to account for that disparity and correct the estimate of the ensemble spread. In this paper, we study the Wang et al. 2007 inflation factor algorithm.

The efficacy of the Wang et al. 2007 inflation algorithm depends on the correlation between the innovations and the observation errors. If positively correlated, the inflation scheme works properly. Otherwise, it is problematic because the contribution from terms involving the ratio of relatively small innovations and large observation errors can make the inflation factor negative. That problem is sometimes addressed by excluding ETKF observations with unreasonably large error estimates.

In this paper, we investigate the sensitivity of the analysis and forecast root mean square error (RMSE), calculated against all radiosonde and synoptic surface observations that pass the WRFDA quality control procedure based on the non-ensemble GSI background forecasts, to changes in the error characteristics of the ETKF observations. Specifically, we study the effect of truncating the lower end of the error distribution by neglecting observations that have relative errors falling below the specified cutoff. We define relative error as the observation error divided by the observation. For reasons discussed in the previous paragraph, the upper end of the distribution is truncated at maximum relative observation error of 20. Our experiments showed that small variations in the maximum error bound did not substantially change the error distribution, but we have not formally investigated that issue.

4. Effect of reducing the number of ETKF observations on the RMSE

In the ETKF, as in the Kalman filter, the resulting ensemble spread increases as the number of ETKF observations decreases. If the ETKF produced the optimal spread for a given number of ETKF observations, one would expect that decreasing the number of ETKF observations would degrade the analysis and the associated forecast. However, due to the disparity between the ensemble size and the number of ETKF observations, the ETKF does not produce the optimal spread, and one might expect a reduction in the number of ETKF observations to enhance the analysis and forecast.

Figure 1 displays the inflation factor time series for experiments that held the number of ETKF observations constant between cycles. The control experiment is identified as WG07 and used the Wang et al. 2007 inflation algorithm with ETKF observations made up of all radiosonde wind, temperature, and moisture observations. WG07 used 20 ensemble members, a variational/ensemble increment weighting, $\beta=0.5$, a horizontal localization, $H=1,500$ km, a vertical localization, $V=20$ grid points 20, and a cycling period of 10 days starting on August 15, 2007. See Mizzi et al. 2011. In Figure 1, R2.5 denotes the use of 2,500 randomly selected ETKF observations per cycle, R5.0 denotes 5,000, R7.5 denotes 7,500, and R10 denotes 10,000. The R() experiments selected their ETKF observations from the WG07 ETKF observations at each cycle. Otherwise, the R() experiments were identical to WG07.

² We refer to the observations entering the ETKF as the “ETKF observations.”

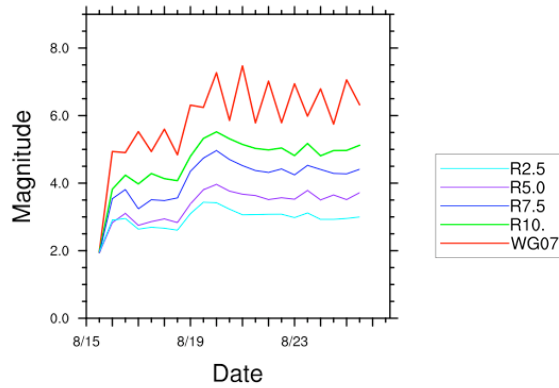


Figure 1. Inflation factor time series for the R2.5, R5.0, R7.5, R10., and WG07 experiments.

Figure 1 shows that WG07 had a bi-cycle oscillation in the inflation factor due to variations in the number of ETKF observations at each cycle. Experiments R2.5 through R10 show that the oscillation disappeared when the number of ETKF observations was held constant. As the relative error cutoff increased, the inflation factor decreased because the initial ensemble spread increased as the number of ETKF observations decreased due to increasing the minimum error cutoff.

The bi-cycle oscillation is also present in ensemble spread time series. See WG07 in Figure 2. Figure 2 displays the ETKF ensemble spread for WG07 and the R() experiments. Figure 2 shows that for WG07: (i) at 00 Z the ETKF ensemble spread was large, when the number of ETKF observations was small $O(15,000)$ (observation number not shown) and (ii) at 12 Z, the ETKF ensemble spread was small, when the number of ETKF observations was large $O(17,000)$ (observation number not shown). However, when the number of ETKF observations was held constant, as in R2.5 through R10, Figure 2 shows that the oscillation disappeared and the inflation factor maintained the target ensemble spread.

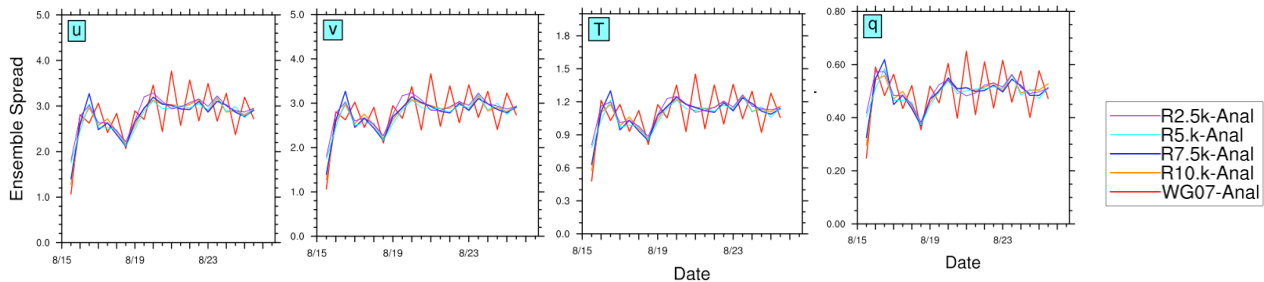


Figure 2. Ensemble spread time series for the R2.5, R5.0, R7.5, R10, and WG07 experiments.

Table 1 displays the analysis and forecast RMSE from WG07 and the R() experiments. The yellow shading identifies the configuration with the lowest forecast RMSE for each meteorological variable. Table 1 shows that reducing the number of ETKF observations improved the analysis and forecast RMSEs, and that the optimal number of ETKF observations ranged between 2,500 and 7,500 and depending on the meteorological variable. However between experiments, the RMSE changes were small and may not be significant. We compared those changes with RMSE changes obtained by increasing the ensemble size from 20 to 80 in increments of 20 (not shown) and found that the changes

UPR	R 2.5	R 5.0	R 7.5	R 10.	WG07
u (m/s)	3.234 (2.323)	3.232 (2.326)	3.230 (2.325)	3.240 (2.324)	3.232 (2.327)
v (m/s)	3.250 (2.363)	3.249 (2.364)	3.251 (2.365)	3.254 (2.362)	3.257 (2.369)
T (K)	1.487 (1.210)	1.484 (1.208)	1.485 (1.207)	1.485 (1.214)	1.491 (1.211)
q (g/kg)	1.297 (0.867)	1.298 (0.872)	1.299 (0.866)	1.302 (0.869)	1.305 (0.870)

Table 1. RMSE for the ETKF observation reduction experiments for non-surface meteorological variables. The forecast RMSE is outside the parentheses, and the analysis RMSE is inside the parentheses. The yellow shading identifies the lowest forecast RMSE for each meteorological variable.

in Table 1 were comparable. Similarly, we compared the RMSE magnitudes and changes in Table 1 to those in Table 2 from Wang et al. 2008b and found that they were comparable. Thus, we conclude that the results in Table 1 are meaningful.

5. Effect of relative observation error filtering of ETKF observations on RMSE

The purpose of this section to investigate whether changing the characteristics of the observation error distribution can improve the analysis and forecast RMSE. Since the goal of the ETKF is to create spread to account for observation uncertainty, and the ETKF misrepresents the spread due to the disparity between the ensemble size and the number of ETKF observations, one might improve the RMSE by retaining observations with relatively large observation errors and excluding those with small errors (assuming that the ETKF underestimates the ensemble spread). Thus, we experiment with varying the minimum relative error cutoff from 0.001 to 1.0 and hold the maximum relative error cutoff constant at 20 (for reasons discussed earlier). We identify the experiment with a minimum relative error cutoff of 0.001 as Ep001, 0.01 as Ep01, 0.1 as Ep1 and 1.0 as E1p. Our experiments showed that setting the minimum cutoff to 2.0 or greater included too few observations in the ETKF.

UPR	E1p	Ep1	Ep01	Ep001	WG07
u (m/s)	3.225 (2.323)	3.222 (2.323)	3.221 (2.320)	3.232 (2.322)	3.232 (2.327)
v (m/s)	3.268 (2.375)	3.252 (2.370)	3.246 (2.365)	3.253 (2.368)	3.257 (2.369)
T (K)	1.477 (1.200)	1.478 (1.205)	1.476 (1.202)	1.489 (1.209)	1.491 (1.211)
q (g/kg)	1.307 (0.868)	1.302 (0.866)	1.300 (0.869)	1.303 (0.867)	1.305 (0.870)

Table 2. RMSE for the minimum relative observation error cutoff experiments for non-surface meteorological variables. The forecast RMSE is outside the parentheses, and the analysis RMSE is inside the parentheses. The yellow shading identifies the lowest forecast RMSE for each meteorological variable.

Table 2 displays the analysis and forecast RMSE for the minimum relative observation error cutoff experiments. The results show that the optimal relative error cutoff was 0.01. The results from Table 1 suggest that the improvements in Table 2 may be due to reducing the number of ETKF observations. However, comparison of RMSE between the two tables shows that Table 2 has lower values for u and v. That suggests that some of the improvement in Table 2 is due to changing the characteristics of the observation error distribution.

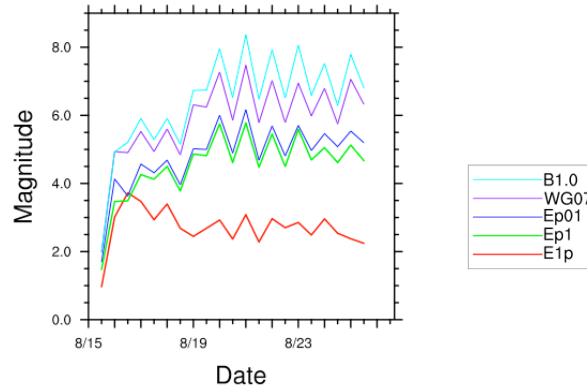


Figure 3. Inflation factor time series for the ensemble/non-hybrid GSI (B1.0), WG07, and selected $E(\cdot)$ experiments.

6. Effect of minimum relative observation error filtering the ETKF observations on inflation, spread, and spread verification

In this section, we examine the effect of observation error filtering on the inflation factors, ensemble spread, and spread verification. Figure 3 shows the effect of filtering on the inflation factors. For all filtering experiments, the inflation factors were smaller than the ensemble/non-hybrid GSI (denoted as B1.0 in Figure 3) and WG07 experiments because the initial ensemble spread decreased as the error cutoff increased.

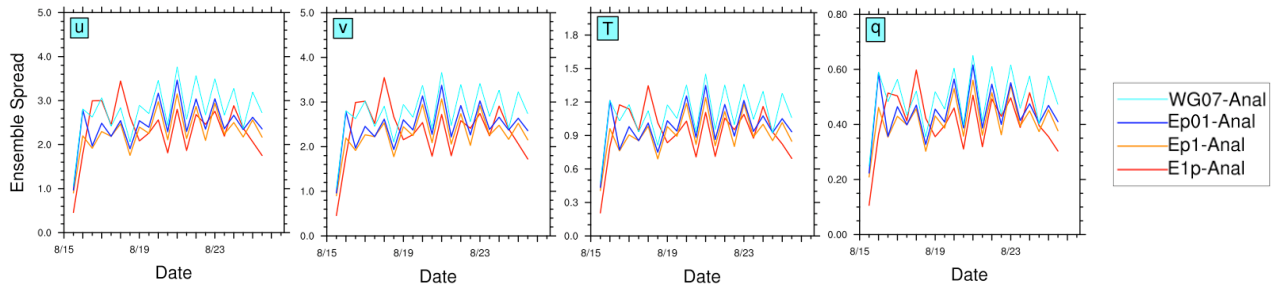


Figure 4. ETKF ensemble spread time series for WG07 and selected $E(\)$ experiments.

Figure 4 shows the ETKF ensemble spread time series for the error filtering experiments. It shows that as the relative error cutoff increased the ensemble spread decreased. That results is counterintuitive. We suspect that the smaller ensemble spread occurred because the inflation factor scheme was unable to maintain the target spread due to averaging and the over/under inflation issue identified by Bowler et al. 2008.

The surprising result from Figure 4 is that the RMSEs in Table 2 improved while the ensemble spread decreased. That suggests that the mechanisms underlying the improvements in Tables 1 and 2 are different. Figure 2 shows that reducing the number of ETKF observation had negligible effect on the ensemble spread, while Figure 4 shows that observation error filtering reduced the spread. Thus, the improvements in Table 1 are likely because: (i) the over/under inflation issue was resolved and (ii) the disparity between the ensemble size and the number of observations was reduced. The cause of the improvements in Table 2 is likely more complex. We speculate that those improvements occur because the final spread is more closely related to background forecast error at the observation locations where the observation uncertainty is greater. If that is correct, then we might expect error filtering to improve the coincidence of the background forecast error and the ETKF ensemble spread.

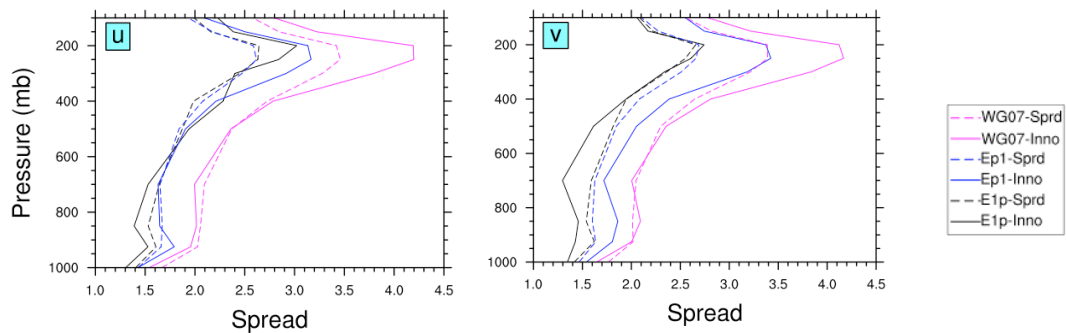


Figure 5. Vertical profiles of the background forecast error (denoted INNO) and the ETKF ensemble spread (denoted SPRD) for WG07 and selected $E(\)$ experiments. The background forecast error is defined as the RMS innovation minus the observation error.

Figure 5 displays vertical profiles of the background forecast error (denoted INNO), defined as the RMS innovation minus the observation error, and the ETKF ensemble spread (denoted SPRD) for u and v from the observation error filtering experiments. Profiles of T and q are not shown because the error filtering excluded all T and q observation points. Figure 5 shows that in the lower and middle troposphere the gaps between the INNO and SPRD profiles for Ep1 and E1p are comparable to that for that for WG07. However, in the upper troposphere, the various experiments have different gaps. WG07 has a gap of ~ 1 m/s at 350 hPa, Ep1 has a gap of ~ 0.6 ms, and E1p has a gap of ~ 0.3 m/s for u and ~ 0.1 m/s for v . In summary, as the minimum observation error cutoff increased, the gap between the INNO and SPRD profiles decreased. Those results suggest that observation error filtering improved the predictive relationship between the ETKF ensemble spread and the background forecast error.

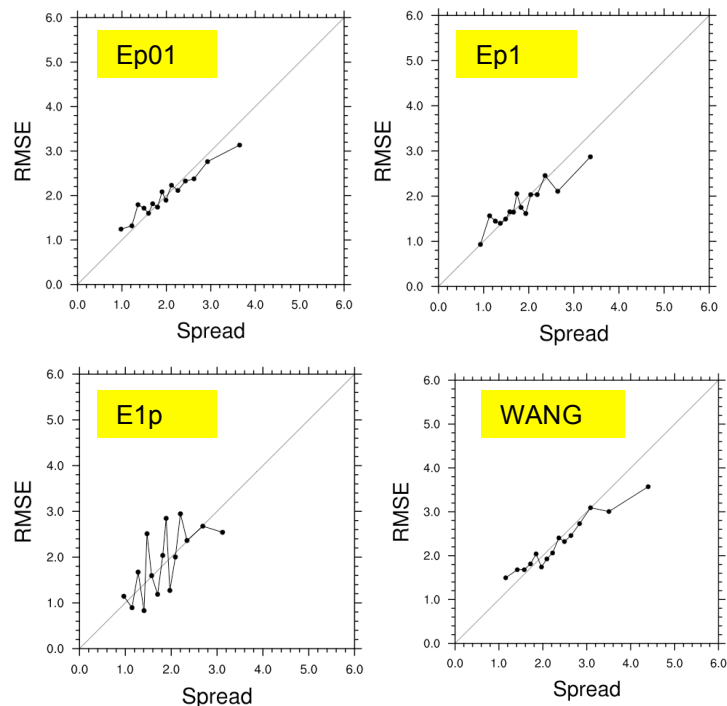


Figure 6. Plots of the background forecast error as a function of ETKF ensemble spread for WG07 and selected $R(\)$ experiments.

Next we look at the effect of error filtering on the ability of the ETKF ensemble spread to distinguish between large and small background forecast errors. We use the method of Majumdar et al. 2001, as applied by Wang et al. 2008a and Wang et al. 2007. We collected u innovation and ensemble spread data from the observation locations at 500 hPa and processed that data according to the procedure of Wang et al. 2008a. We used 15 bins, and the numbers of points per bin were as follows: 130 for WG07, 90 for Ep01, 85 for Ep1, and 8 for E1p. Ideally, the plotted points should fall along the 45° line. The results are displayed in Figure 6.

Figure 6 shows that for all experiments the adjusted innovation/ensemble spread pairs fall along the 45° line, and that the results from the R() experiments generally agree with those from WG07. The results for E1p display greater variability about the 45° line because the number of points per bin is too small to get representative results. Figure 6 suggests that error filtering did not negatively impact the ability of the ETKF ensemble spread to distinguish between large and small background errors.

Finally, we examine the RMSE and bias from verification of the observation error filtering experiments. The RMSEs are displayed in Figure 7, and the biases are in Figure 8. Figure 7 shows that error filtering had no material effect on RMSE. Figure 8 shows that there was: (i) a reduction in the forecast bias for u in the upper troposphere, (ii) a reduction in the forecast bias for T in the middle and upper troposphere, and (iii) a reduction in the forecast bias for q in the middle and lower troposphere. For v , there was a small increase in the forecast bias throughout the troposphere. The changes to the analysis bias were similar but quantitatively smaller.

7. Discussion and conclusions

In this paper, we studied the effects of changing the ETKF observation error characteristics in the GSI/ETKF regional hybrid on the analysis and forecast RMSE. As part of that study, we investigated the effects of: (i) reducing the number of ETKF observations and (ii) holding the number of ETKF observations constant between cycles.

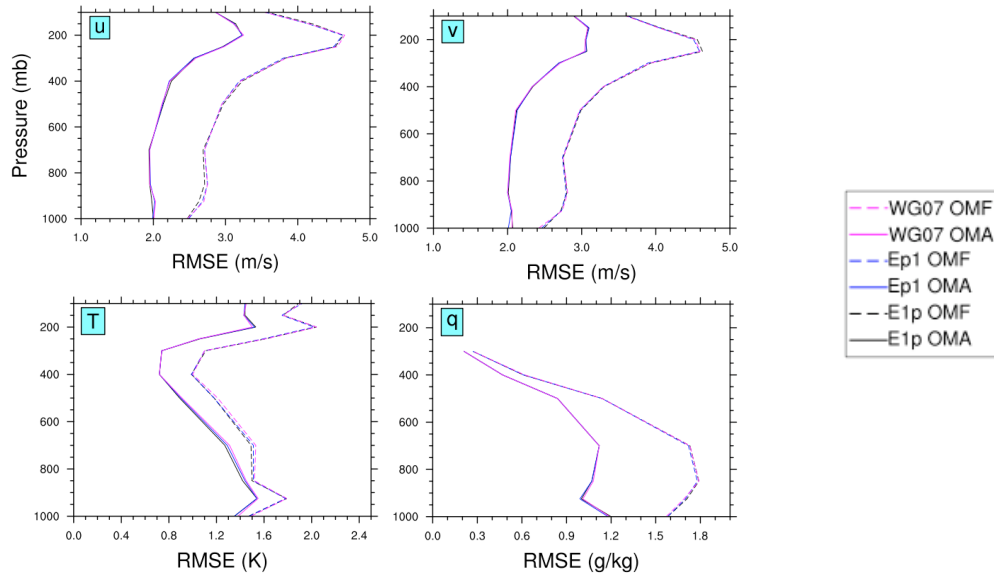


Figure 7. Vertical profiles of the RMSE for WG07 and selected E() experiments. The analysis RMSEs are identified with OMA and the forecast RMSEs with OMF.

Our results showed that reducing the number of ETKF observations improved the analysis and forecast RMSE. We found that the optimal number of ETKF observation ranged between 2,500 and 7,500 depending on the meteorological variable. We found that the ETKF ensemble spread was not affected by changing the number of ETKF observations because the inflation factor scheme compensated for the spread reduction associated with reducing the number of ETKF observations. We speculate that the optimal number of ETKF observations is application dependent. Here we used a coarse domain, limited the ETKF observations to radiosonde u, v, T, and q data, and used a single inflation factor for all meteorological variables. If the resolution were changed, the optimal number of ETKF observations would likely change. If the types of ETKF observations were changed, for example by including all conventional observations, then the optimal number of observations would likely be dependent on the error characteristics of the different observation platforms. If separate inflation factors were used for each meteorological variable, we interpret our results as indicating that the optimal number of ETKF observations would be different for wind (u,v), T, and q. That suggests that the ETKF and inflation factor should be applied separately to each variable.

Our results showed that: (i) the bi-cycle oscillation in the inflation factor and ensemble spread was due to variations in the number of ETKF observations at the different cycle times and (ii) holding the number of ETKF observations constant between cycles eliminated those oscillations. We speculate that the inflation factor was unable to correct the oscillations in WG07 due to the averaging, *see* Wang et al. 2007 and due to the over/under inflation identified by Bowler et al. 2008.

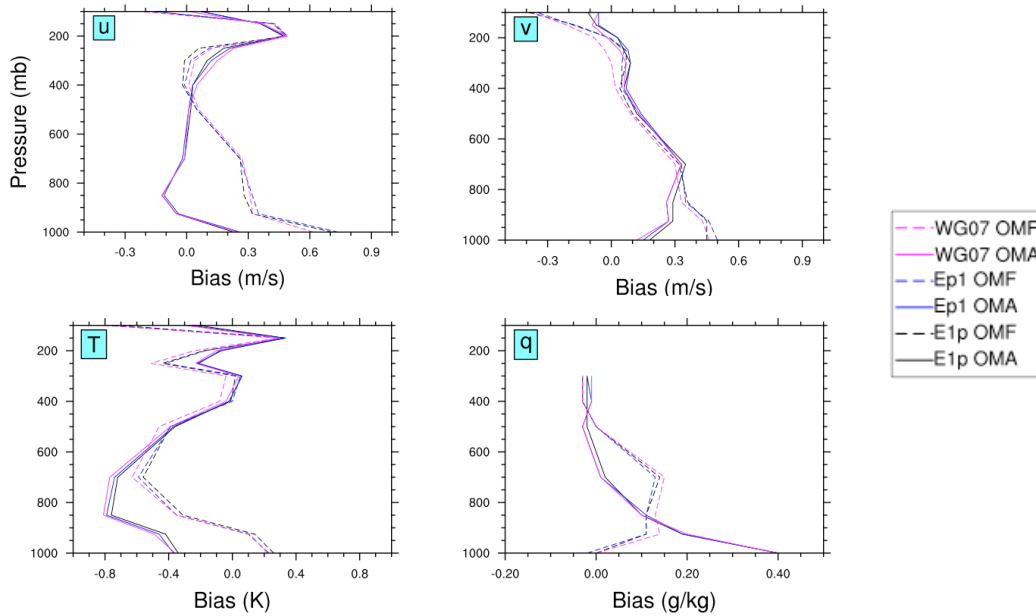


Figure 8. Vertical profiles of the bias for WG07 and selected E() experiments. The analysis biases are identified with OMA and the forecast biases with OMF

When the number of ETKF observations was held constant between cycles, the inflation factor scheme properly maintained the target ensemble spread from one cycle to the next even when the number of observations was reduced from one experiment to another.

Our results showed that changing the characteristics of the observation error distribution by using a minimum relative observation cutoff, which altered the mean, variance, and skewness of the distribution, had a beneficial effect on the analysis and forecast RMSE. We found that the optimal minimum relative error cutoff was 0.01. That result is likely to be application dependent. We found that the RMSE improved when the minimum relative error cutoff was increased and the ensemble spread decreased. That result is counterintuitive. For the relative error filtering experiments, we suspect that the ensemble spread decreased because the inflation factor scheme could not maintain the target spread due to averaging and the over/under inflation issue. We recommend rerunning those experiments with the number of ETKF observation held constant.

We speculate that the improvements from holding the number of ETKF observation constant occurred because: (i) the over/under inflation issue was resolved and (ii) the disparity between the ensemble size and the number of ETKF observations was reduced. The improvements from increasing the minimum relative observation cutoff were likely because filtering more closely related the background forecast error and ensemble spread at locations where the observation uncertainty was greater. That explanation is supported by vertical profiles of background forecast error and ensemble spread which showed that error filtering reduced the gap between those profiles in the upper troposphere (where the has been characteristically large) without negatively impacting the ability of the ensemble spread to distinguish between large and small background forecast errors.

8. References

Bishop, C.H., B.J. Etherton, and S.J. Majumdar, 2001: Adaptive sampling with the ensemble transform Kalman filter. Part I: Theoretical Aspects. *Mon. Wea. Rev.*, **129**, 420-436.

Bowler, N.E., A. Arribas, K.R. Mylne, K.B. Robertson, and S.E. Beare, 2008: The MOGREPS short-range ensemble prediction system. *Quart. J. Meteor. Soc.*, **134**, 703-722.

Majumdar, S.J., C.H. Bishop, B.J. Etherton, I. Szunyogh, and Z. Toth, 2001: Can an ensemble transform Kalman filter predict the reduction in forecast error variance produced by targeted observations? *Quart. J. Meteor. Soc.*, **127**, 2803-2820.

Mizzi, A.P., Z. Liu, and X.Y. Huang, 2011: A hybrid GSI/ETKF data assimilation scheme for WRF/ARW. 15th Symposium on Integrated Observing and Assimilation Systems for the Atmosphere, Oceans, and Land Surface; and the 24th Conference on Weather and Forecasting/20th Conference on Numerical Weather Prediction (J16.1), January 23-27, 2011, Seattle, Washington.

Wang, X., 2010: Incorporating ensemble covariance in the gridpoint statistical interpolation variational minimization: A mathematical framework. *Mon. Wea. Rev.*, **138**, 2990-2995.

Wang, X., and C.H. Bishop, 2003: A comparison of breeding and ensemble transform Kalman filter ensemble forecasts schemes. *J. Atmos. Sci.*, **60**, 1140-1158.

Wang, X., T.M. Hamill, J.S. Whitaker, and C.H. Bishop, 2007: A comparison of hybrid ensemble transform Kalman filter-OI and ensemble square-root filter analysis schemes. *Mon. Wea. Rev.*, **135**, 1055-1076.

Wang, X., D.M. Barker, C. Snyder, and T.M. Hamill, 2008a: A hybrid ETKF-3DVAR data assimilation scheme for the WRF model, Part I: Observing system simulation experiment. *Mon. Wea. Rev.*, **136**, 5116-5131.

Wang, X., D.M. Barker, C. Snyder, and T.M. Hamill, 2008b: A hybrid ETKF-3DVAR data assimilation scheme for the WRF model, Part II: Real observation experiment. *Mon. Wea. Rev.*, **136**, 5132-5147.